Very Long Wavelength $In_xGa_{1-x}As/GaAs$ Quantum Well Infrared Photodetectors

S. D. Gunapala

Center for Space Microelectronics Technology, Jet Propulsion Laboratory, California Institute of Technology, Pasadena,CA91109

K. M. S. V. Bandara, B. F. Levine, G. Sarusi, D. L. Sivco, A. Y. Cho

AT&T Bell Laboratories, Murray Hill, NJ 07974

ABSTRACT

We demonstrate the first long-wavelength (Xc= **20 pm)** quantum well infrared photodetector using non-lattice matched $In_xGa_{1-x}As/GaAs$ materials system. High optical gains (low capture probabilities) were achieved by using GaAs as a barrier material in this system. The detectivity has been found to be comparable to those achieved with the usual lattice matched $GaAs/Al_xGa_{1-x}As$ detectors.

High performance $GaAs/Al_xGa_{1-x}As$ quantum-well infrared photodetectors (QWIPs) as well as large staring arrays that operate in the long-wavelength spectral region $\lambda = 7$-12 μm [1-15] have been demonstrated. However, longer-wavelength detectors arc required for a variety of application including many advanced NASA satellite missions. These space applications have placed stringent requirements on the performance of the IR detectors and arrays such as high detectivity, low dark current, high uniformity, radiation hardness and lower power dissipation. There is a additional interest in these very long-wavelength is duc to the fact that this spectral region is rich in information vital to the understanding of composition, structure and the energy balance of molecular clouds and stars forming regions of our galaxy. Therefore, NASA has great interest in infrared detectors both inside and outside the atmospheric windows (3-5 μm and 8-12 pm). This paper will present a study and development of a low-dark-current very long-wavelength $In_xGa_{1-x}As/GaAs$ QWIPs.

For all of the GaAs based QWIPs which have been demonstrated thus far, GaAs is the low bandgap *well* material and the barriers are *lattice matched* $Al_xGa_{1-x}As$, $Ga_{0.5}In_{0.5}P$ or $Al_{0.5}In_{0.5}P$. However, it is interesting to consider GaAs as the *barrier* material since the transport in binary GaAs is expected to be superior to that of a ternary alloy, as was previously found to be the case in the $In_{0.53}Ga_{0.47}As/InP$ binary barrier structures [4,5]. To achieve this, we have used the lower bandgap non-lattice matched alloy $In_xGa_{1-x}As$ as well material together with GaAs barriers. It has been demonstrated 16!17 that strain layer heterostructures can be grown for lower In concentrations ($x < 0.15$) which results in lower barrier heights. Therefore, this heterobarrier system is very suitable for very long-wavelength ($\lambda > 14\ \mu m$) QWIPS.

The samples were grown on semi-insulating GaAs substrates by molecular beam epitaxy. The first structure shown in Fig. 1(a) consisted of 5 sets of 80 Å $In_{0.15}Ga_{0.85}As$ quantum wells doped $N_D = 5 \times 10^{17}\ cm^{-3}$ separated by 500 Å barriers of undoped GaAs, with the top and bottom contacts being $N_D = 1 \times 10^{18}\ cm^{-3}$ doped GaAs. It should be noted that unlike all the other QWIPs demonstrated thus far, in this structure the heavily doped contacts arc made using the *high* band gap (i.e. GaAs) semiconductor. This is quite different from the $GaAs/Al_xGa_{1-x}As$ heterosystem in which the GaAs is the low bandgap quantum well and contact material. This reversal

for the $In_{0.15}Ga_{0.85}As/GaAs$ structure is necessary since a thick contact layer of the strained non-lattice matched $In_{0.15}Ga_{0.85}As$ material would have too many defects and threading dislocations. The design shown in Fig. 1(a) overcomes this problem by making use of the strong band bending between the heavily doped GaAs contact layers and the first and last $In_{0.15}Ga_{0.85}As$ quantum wells. This results in a large tunneling current (schematically indicated by the double arrow in Fig. 1(a), which essentially "short circuits" the first and last wells, thus effectively contacting the low bandgap material. The active QWIP structure therefore consists of the central *three* quantum wells.

The second structure, schematically shown in Fig. 1(b) is slightly different from the first structure consisted of 3 sets of 85 Å $In_{0.15}Ga_{0.85}As$ quantum wells doped $N_D = 1 \times 10^{17}\ cm^{-3}$ separated by two 500 Å barriers of undoped GaAs, with the top and bottom contacts being $N_D = 1 \times 10^{17}\ cm^{-3}$ doped GaAs. Also this structure has two additional undoped GaAs spacer layers bctwccn the quantum wells and the top and bottom contact layers. As a result of these undoped spacer layers and the lower contact doping, the tunneling injection current from contacts to the quantum wells expected to be smaller in this structure in comparison to the first structure.

All of the QWIPs were processed into 200 μm diameter mesas (area = 3.14 x 10-4 cm^2) using wet chemical etching and Au/Ge ohmic contacts were evaporated onto the top and bottom contact layers. The dark current voltage curves for both samples were measured as a function of temperature from T = 30-60 K as shown in Fig. 2. As expected, Fig. 2 clearly shows that the dark current of the second structure is many orders of magnitude smaller than the dark current of the first structure for temperatures up to 60 K (dark current of the first structure at 60 K is out of range of Fig. 2) which indicates that the undoped spacer layers and the lower contact doping significantly reduced the tunneling injection current to the quantum wells. As a result the second structure is background-limited at a much higher temperature than the first structure. Note the reduced asymmetry in the dark current $^{18}I_D$ of this device structures. This attributes to the lower well doping (higher well doping will increase the dopant diffusion into the growth direction and hence higher asymmetry in the band structure).

The responsivity spectra of these 200 μm diameter mesa detectors were measured using a 1000 K blackbody source and a grating monochromator. The detectors were back illuminated through a 45° polished facet[1] and their responsivity spectrums are shown in Fig. 3. The responsivities of the first and the second structures peak at 15.3 μm and 17.5 μm respectively. The peak responsivities (R_p) of the first and the second samples are 300 and 63 mA/W respectively at bias V_B = 100 mV. The spectral widths and the cutoff wavelengths are $\Delta\lambda / \lambda$ = 50% and λ_c = 18.3 μm for the first structure and $\Delta\lambda / \lambda$ = 11% and λ_c = 20 μm (corrected for substrate absorption) for the second structure. The higher peak wavelength λ_p = 17.5 μm of the second sample is attributed to the slightly wider well width. These peak wavelengths and the spectral widths are in good agreement with theoretical estimates of bound-to-continuum intersubband transition based on the InO.15Gaog5As/GaAs band offset. Note that the sharp drop in responsivity of the second structure at longer wavelength (λ > 18 μm) is duc to strong multi-phonon process in GaAs substrate which starts to absorb near λ = 18 μm [2]. Thus, the measured cutoff wavelength of the second structure is determined by the substrate absorption and not by intrinsic QWJP photo response. Therefore, the corrected (for substrate absorption) cutoff wavelength of the second structure is λ_c = 20 μm. The absolute peak responsivities (R_p) of the detectors were measured using a calibrated blackbody source and results are shown in Fig. 4, The measured absolute responsivities of both samples increase nearly linearly with the bias reaching Rp = 500 and 151 mA/W at V_B = 150 mV for the first and the second device structures respectively. The lower rcsponsivity of the second sample is due to the factor of five lower doping density in the second sample.

The current noise in was measured using a spectrum analyzer and experimentally determined the optical gain g using $i_n = \sqrt{4eI_D g\Delta f} + 1/2N$. As shown in Fig. 5, optical gains of the first and second structures reached 10.5 and 8.5 at V_B = 100 and 220 mV respectively which is very large compare to usual $Al_xGa_{1-x}As/GaAs$ QWIPs. Since the gain of QWIP is proportional to the number of quantum wells N, the better comparison would be the well capture probability p_c, which is directly related to the gain by g = $1/Np_c$. The calculated well capture probabilities arc 16% at low bias and 3% at high bias voltage which indicate the excellent hot-electron transport in this device structures. This may be a result of the high mobility binary GaAs barriers. The peak dctectivity D* can now be calculated from $D^* = R\sqrt{A\Delta f}/i_n$, where A is the area of the detector and A

= 3.14x10-4 cm^2. Table 1 shows the D* values of both device structures at various temperatures at a bias of V_B = 100 mV. The detectivity of the first device structure could not be measured at T = 50 K due to the higher dark current. The detectivity values in the Table 1 clearly show the advantage of the undoped spacer layer which reduces the dark current by many orders of magnitude (and hence corresponding increase in the defectivity).

In summary, we have demonstrated the first very long-wavelength (λ_C = 20 μm) $In_xGa_{1-x}As/GaAs$ QWIP. The large responsivity and detectivity D* values arc comparable to those achieved with the usual lattice matched $GaAs/Al_xGa_{1-x}As$ materials system. The high optical gains and the small carrier capture probabilities demonstrate the excellent carrier transport of the GaAs barriers and the potential of this heterobarrier system for very long-wavelength ($\lambda > 14$ pm) QWIPs.

We are grateful to C. A. Kukkonen, V. Sarohia, S. Khanna, K. M. Koliwad, B. A. Wilson, and P. J. Grunthaner of the Jet Propulsion Laboratory for encouragement and support of this work. The research described in this paper was performed by the Center for Space Microelectronics Technology, Jet Propulsion Laboratory, California Institute of Technology, and was jointly sponsored by the Ballistic Missile Defense Organization/Innovative Science and Technology Office, and the National Aeronautics and Space Administration, Office of Advanced Concepts and Technology,

REFERENCES

1. B, F. Levine, C. G. Bethea, G. Hasnain, J. Walker, and R. J. Malik, Appl. Phys. Lett. 53.(1988) 296.
2. B. F. Levine, *Proceedings of the NATO Advanced Research Workshop on Intersubband Transitions in Quantum Wells,* Cargese, France Sept. 9-14, 1991, edited by E. Rosencher, B. Vinter, and B. F. Levine (Plenum, London, 1992).
3. J. Y. Andersson and L. Lundqvist, Appl. Phys. Lett. 59,857 (1991).
4. S. D. Gunapala, B. F. Levine, D. Ritter, R. A. Harem, and M. B. Panish, Appl. Phys. Lett. 58,2024 (1991).
5. S. D. Gunapala, B. F. Levine, D. Ritter, R. A. Harem, and M. B. Panish, Appl. Phys. Lett. 60,636 (1992).
6. B. K. Janousek, M, J. Daugherty, W. I.. Bless, M. L. Rosenbluth, M. J. O'Loughlin, H. Kanter, F. J. De Luccia, and L. E. Perry, J. Appl. Phys. 67,7608 (1990).
7. S. R. Andrews and B. A. Miller, J. Appl. Phys. 70,993 (1991).
8. L. S. Yu and S. S. Li, Appl. Phys. Lett. 59, 1332 (1991).
9. A. G. Steele, H. C. Liu, M. Buchanan, and Z. R. Wasilewski, Appl. Phys. Lett. 59, 3625 (1991).
10. S. D. Gunapala, B. F. Levine, L. Pfeiffer, and K. West, J. Appl. Phys. 69, 6517 (1990).
11. M. J. Kane S. Millidge, M. T. Emeny, D. Lee, D. R. P. Guy, and C. R. Whitehouse in Ref. 2,
12. C. S. Wu, C. P. Wen, R. N. Sate, M, Hu, C. W. Tu, J. Zhang, L. D. Flesner, L. Pham, and P. S. Nayer, IEEE Tran. Electron Devices *39,234 (1992).*
13. B. F. Levine, C. G. Bethea, K. G. Glogovsky, J. W. Stayt, and R. E. Labenguth, Semicon. Sci. Technol. 6(1 991) cl 14.
14. M. T. Asom et al., Proceedings of the IRIS Specialty Group on Infrared Materials, Boulder, CO, August 12-16,1991, Vol. 1, p. 13.
15. L. J. Kozlowski, G, M. Williams, G. J. Sullivan, C. W. Farley, R. J. Anderson, J. K. Chen, D. T. Cheung, W. E. Tennant, and R. E. DeWames, IEEE Trans. Electron Devices 38, 1124 (1991).
16. X. Zhou, P. K. Bhattacharya, G. Hugo, S. C. Hong and E. Gulari, Appl. Phys. Lett. 54,855 *(1989).*

17. B. Elman, E. S. Koteles, P. Melman, C. Jagannath, J. Lee and D. Dugger, Appl. Phys. Lett. 55, 1659 (1989).
18. A Zussman, B. F. Levine, J. M. Kuo and J. de Jong, J. Appl. Phys. 70,5101 (1991).
19. The well capture probabilities (P_c) were calculated from $g = 1/NP_c$, where N is the number of quantum wells.

TABLE I. Comparison of detectivities with and without undoped spacer layers.

T (K)	D* (cm√Hz/W) no spacer layer	D* (cm√Hz/W) with spacer layer
10	8.0×10^{9}	9.7×10^{10}
30	7.8×10^{7}	2.1×10^{9}
40	4.0×10^{7}	1.1×10^{9}
50		1.3X108

FIGURE CAPTIONS

Fig. 1 (a) Conduction-band diagram of the first $In_{0.15}Ga_{0.85}As/GaAs$ QWIP structure. (b) Conduction-band diagram of the second $In_{0.15}Ga_{0.85}As/GaAs$ QWIP structure. Unlike the first structure, this structure has two additional undoped GaAs spacer layers between the quantum-wells and the top and bottom contact layers.

Fig. 2 Dark current versus bias voltage at two different temperatures for the first and the second device structure. This clearly indicates the reduction of dark current as a result of spacer layers which reduces the current injection into the photosensitive multi quantum well region.

Fig. 3 Responsivity spectrums of the first (dashed) and the second (solid) samples measured at T = 40 K.

Fig. 4 Bias dependent peak responsivities of the first and the second samples measured at T=40K.

Fig. 5 Optical gain versus bias voltage for both device structures at temperature T =40 K.

(a)

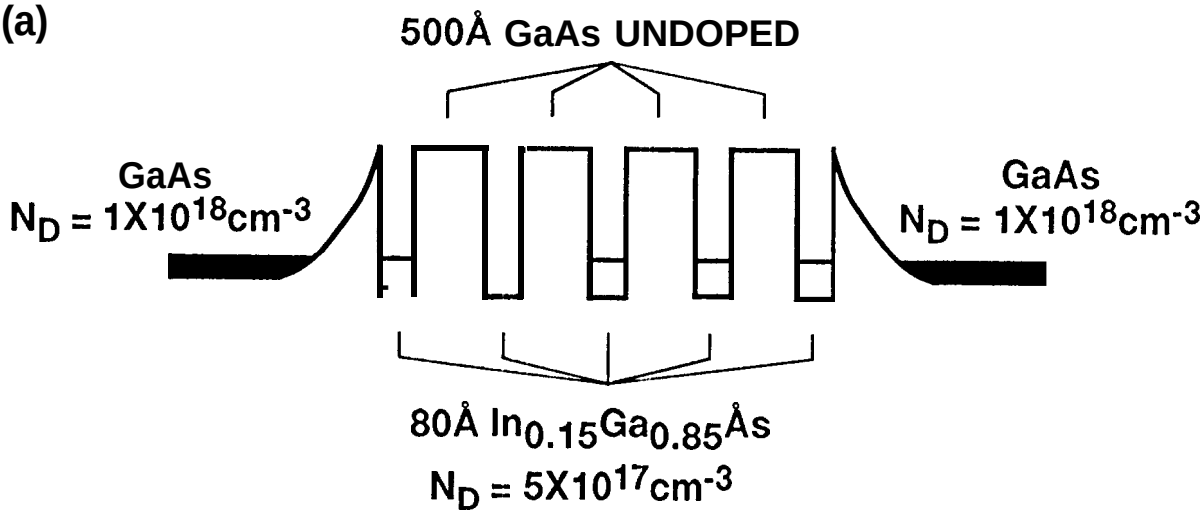
500Å GaAs UNDOPED
GaAs
$N_D = 1X10^{18}cm^{-3}$
GaAs
$N_D = 1X10^{18}cm^{-3}$
80Å $In_{0.15}Ga_{0.85}As$
$N_D = 5X10^{17}cm^{-3}$

(b)

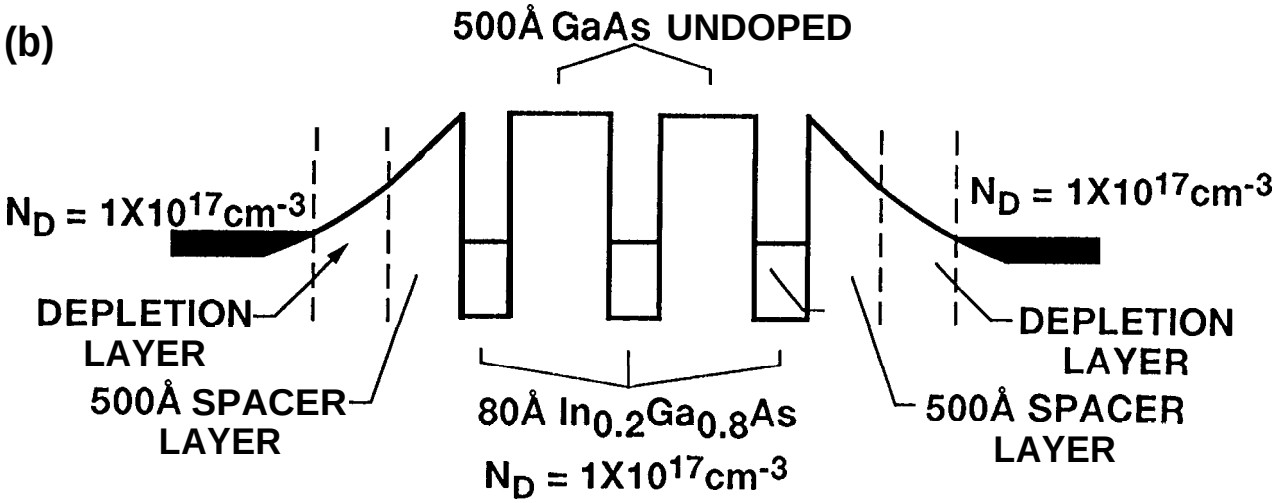
500Å GaAs UNDOPED
$N_D = 1X10^{17}cm^{-3}$
$N_D = 1X10^{17}cm^{-3}$
DEPLETION LAYER
500Å SPACER LAYER
80Å $In_{0.2}Ga_{0.8}As$
$N_D = 1X10^{17}cm^{-3}$
500Å SPACER LAYER
DEPLETION LAYER

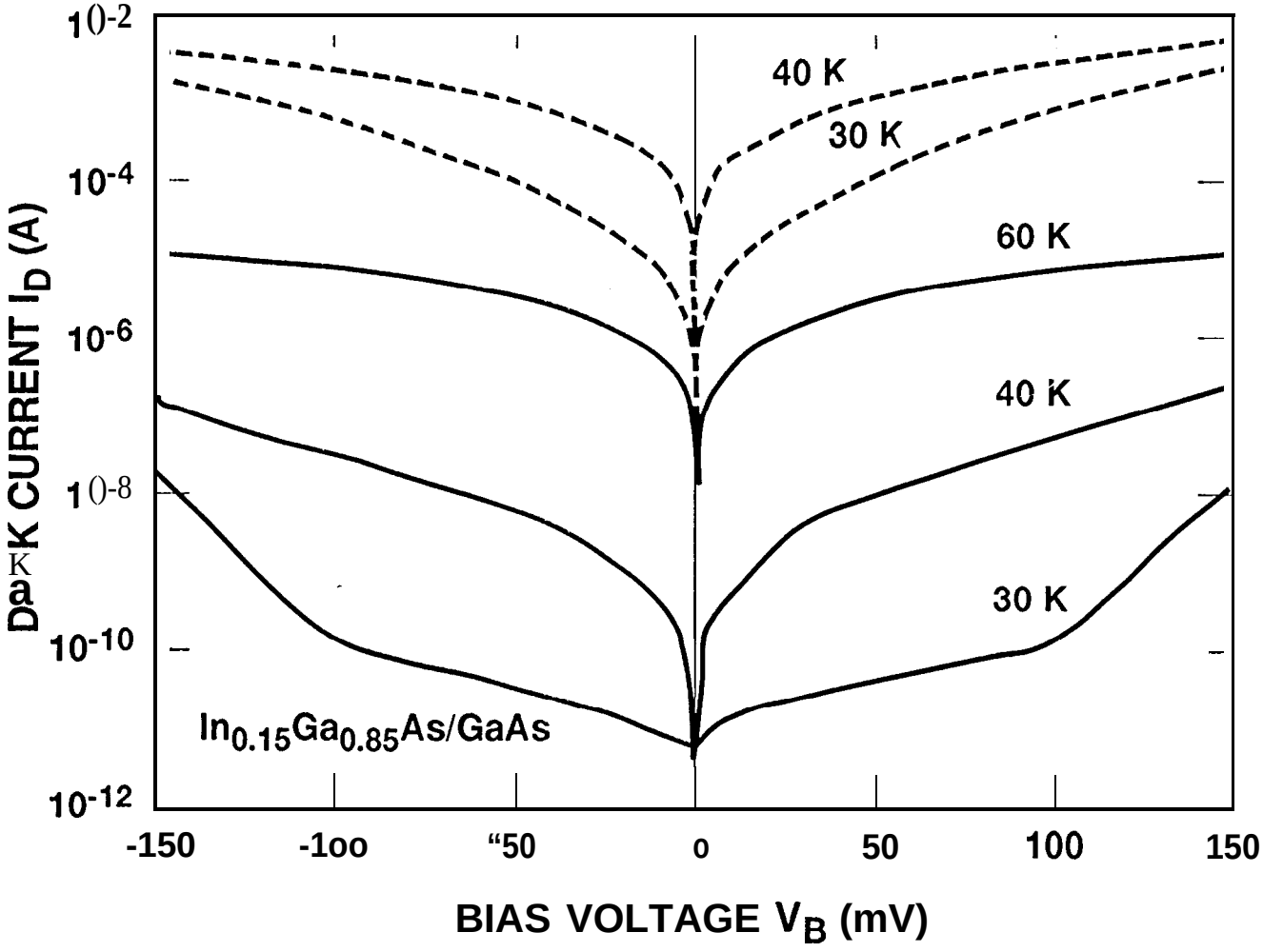
10-2
10-4
10-6
10-8
10-10
10-12
DARK CURRENT ID (A)
40 K
30 K
60 K
40 K
30 K
In0.15Ga0.85As/GaAs
-150
-100
-50
0
50
100
150
BIAS VOLTAGE VB (mV)

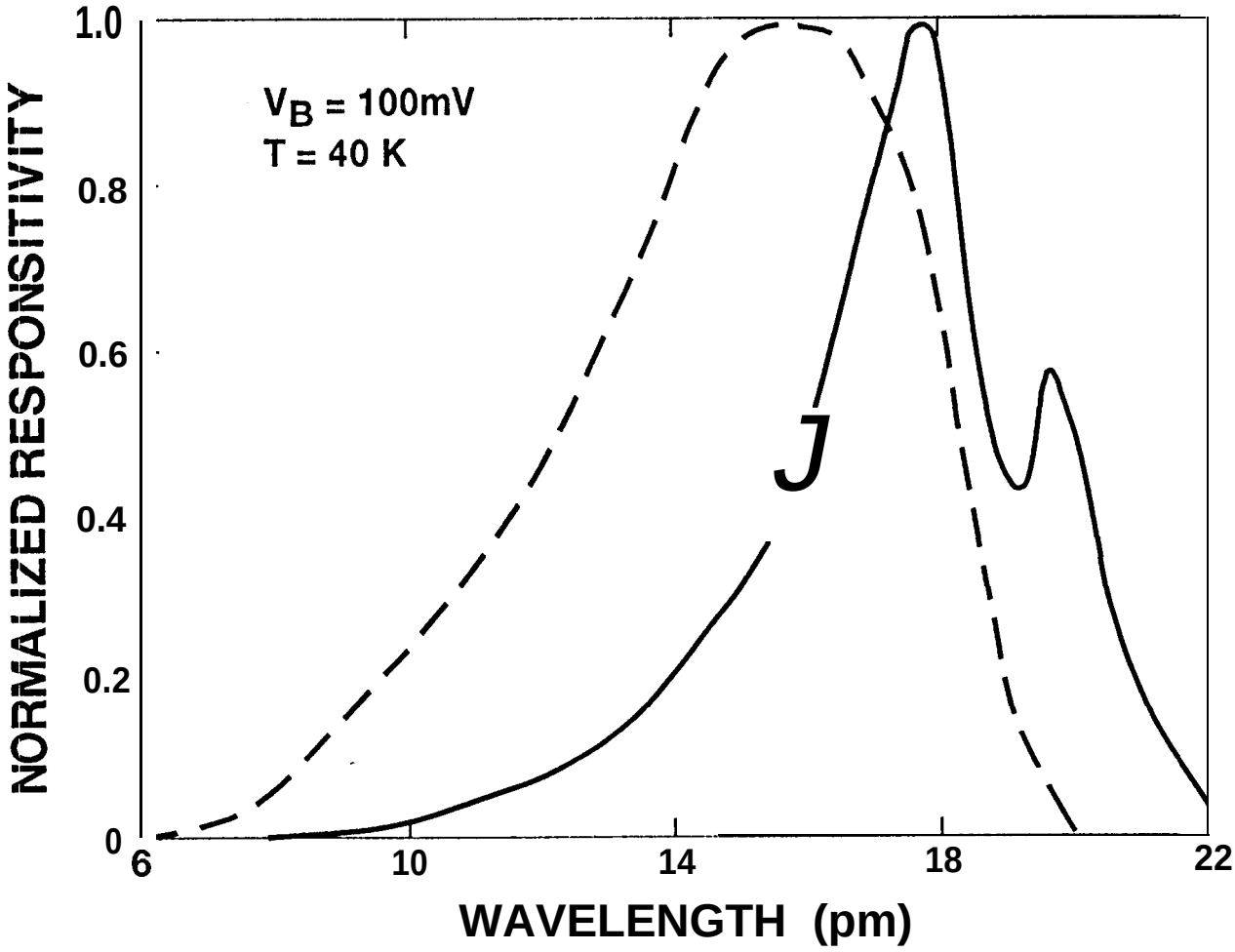
1.0
0.8
0.6
0.4
0.2
0
NORMALIZED RESPONSITIVITY
V_B = 100mV
T = 40 K
J
6
10
14
18
22
WAVELENGTH (pm)

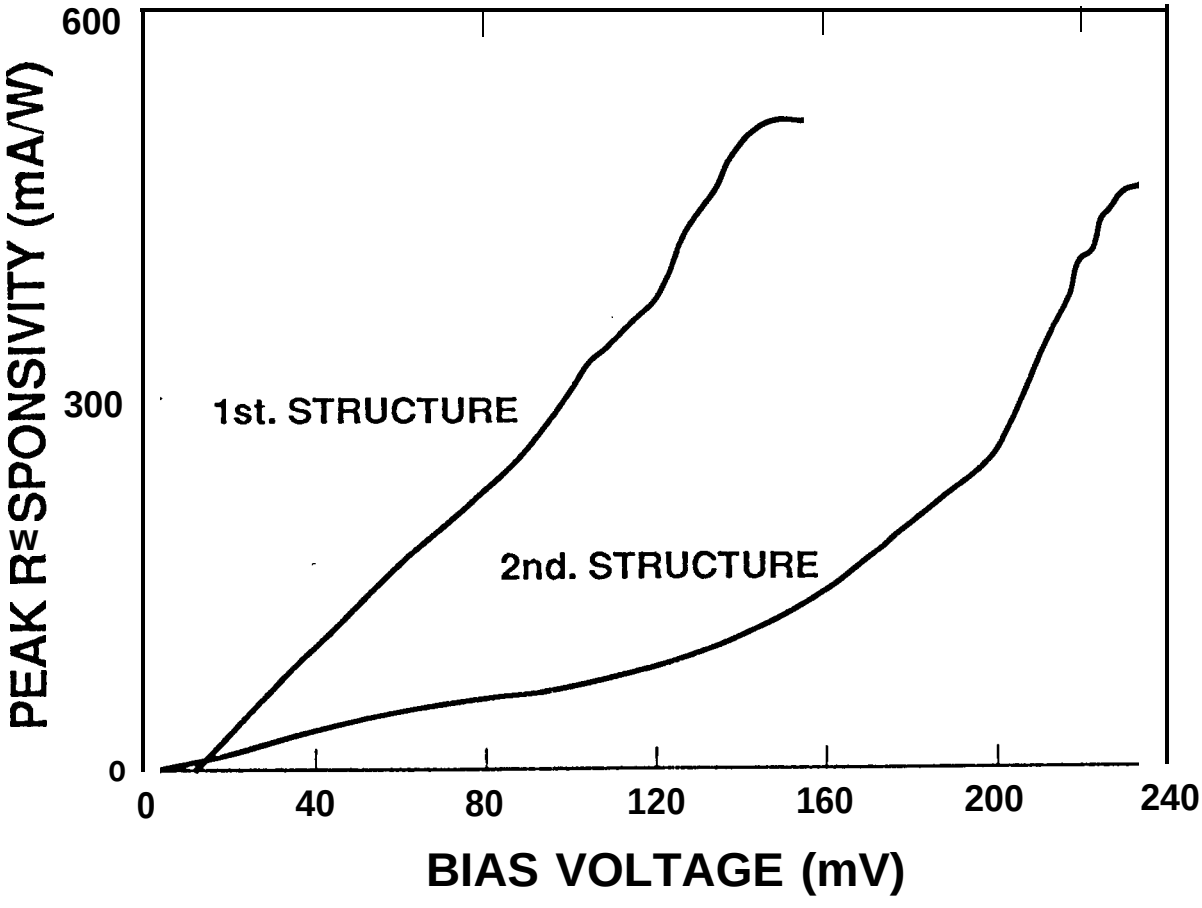
600
300
0
PEAK RESPONSIVITY (mA/W)
1st. STRUCTURE
2nd. STRUCTURE
0
40
80
120
160
200
240
BIAS VOLTAGE (mV)

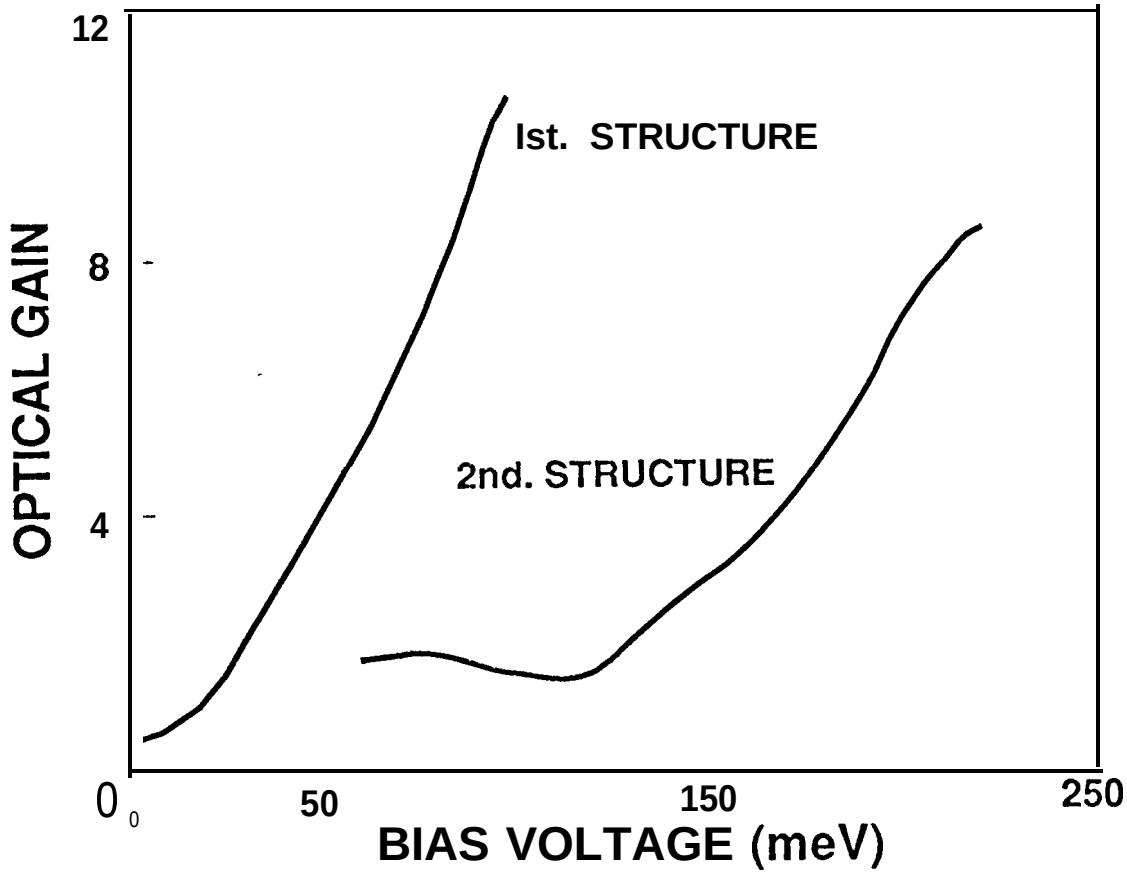
12
8
4
0
OPTICAL GAIN
1st. STRUCTURE
2nd. STRUCTURE
0
50
150
250
BIAS VOLTAGE (meV)